



COUPLED FLEXURAL–TORSIONAL VIBRATIONS OF TIMOSHENKO BEAMS

A. N. BERCIN AND M. TANAKA

*Department of Mechanical Systems Engineering, Shinshu University, 500 Wakasato,
Nagano 380, Japan*

(Received 5 October 1996, and in final form 23 April 1997)

A study of the coupled flexural–torsional vibrations of monosymmetric beams is presented. The effects of warping stiffness, shear deformation and rotatory inertia are taken into account in the formulations. Numerical results are given for three cantilever beams both including and excluding the effects of warping stiffness. It is seen that as the modal index and the thickness of the beam increase, shear deformation, rotatory inertia and warping effects become more pronounced on the natural frequencies, and therefore the errors can be unacceptably large if these effects are ignored.

© 1997 Academic Press Limited

1. INTRODUCTION

Beams are basic structural elements which have found widespread use in most branches of structural engineering. It is now well known that when the beam cross-section has two axes of symmetry, centroid and shear center coincide. The two flexural vibrations and torsional vibration of such beams are independent. However, if the beam cross-section has a single axis of symmetry, the centroid and shear center are separated by a distance which results in coupling between flexural vibration in the perpendicular direction of the symmetry axis and torsional vibration.

Although a voluminous literature exists concerning the vibrational characteristics of beams having two axes of symmetry, the number of studies dealing with coupled flexural–torsional vibrations of beams is rather limited. A comprehensive historical survey of coupled vibrations of beams was presented by Friberg [1] in 1983. Since then, several works have appeared in the literature. These investigations can be broadly classified into three groups, based on the various beam theories used in the formulations.

(i) *Euler–Bernoulli Theory*. Neglecting the effect of warping, Dokumaci [2] determined the coupled free vibrational frequencies of a cantilever beam. His theory was extended to include warping by Bishop *et al.* [3], who demonstrated that omission of warping effects leads to considerable errors in the coupled frequencies of open section beams. Later, Banerjee *et al.* [4] recast the approach of reference [3] in the form of dynamic stiffness matrix. Banerjee and associates [5–8] made notable contributions to the solution of the problem. They gave allowance to the presence of axial force and also presented explicit algebraic expressions for the terms of the dynamic stiffness matrix which are usually obtained numerically due to the complicated nature of the problem. Recently, Klausbruckner and Pryputniewicz [9] investigated the vibrational characteristics of channel beams using laser hologram interferometry. Tanaka and Bercin [10] employed a symbolic manipulation package in the determination of coupled frequencies of asymmetric cross-section beams.

(ii) *Vlasov Theory*. Examples of literature within this group are given by Friberg [11] and Leung [12, 13], both of whom used the dynamic stiffness method and considered the effect of static axial force. A finite element formulation of the problem has been reported by Dvorkin *et al.* [14].

(iii) *Timoshenko Theory*. Coupled bending–torsional vibrations of Timoshenko beams have been studied by Bishop and Price [15] and, more recently, by Banerjee and Williams [16], who later took into account the effect of axial loading [17]. In all of these works, warping stiffness has been neglected.

The aim of the present study is twofold. It has been shown earlier [3] that allowance for warping can make great differences to coupled frequencies of open section beams. For this reason, the first objective is to include the effect of warping in the coupled vibration analysis of Timoshenko beams. Although the coupled vibrations of Timoshenko beams are solved in elegant ways in references [15] and [16], numerical results are not provided. Therefore, the second aim is to present some accurate data which might be useful for other researchers to compare their results. To this end coupled bending–torsional frequencies of monosymmetric beams are given for clamped–free boundary conditions by excluding and including the effect of warping.

2. FORMULATION OF THE PROBLEM

A typical thin-walled monosymmetric beam of length L is depicted in Figure 1. The centroid and shear center are denoted by C and S , respectively, and are separated by a distance e . The flexural translation in the y direction, the bending slope and torsional rotation about the x -axis are represented by $v(x, t)$, $\theta(x, t)$ and $\phi(x, t)$, respectively. The differential equations for coupled vibrations of a Timoshenko beam may be written in the form

$$kGA\left(\frac{\partial^2 v}{\partial x^2} - \frac{\partial \theta}{\partial x}\right) - m \frac{\partial^2 v}{\partial t^2} + em \frac{\partial^2 \phi}{\partial t^2} = 0, \quad (1)$$

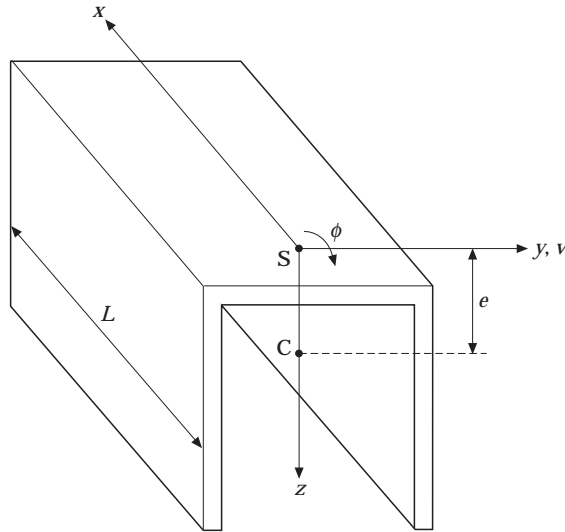


Figure 1. The co-ordinate system and geometric parameters of a monosymmetric beam.

$$EI \frac{\partial^2 \theta}{\partial x^2} + kGA \left(\frac{\partial v}{\partial x} - \theta \right) - I_c \frac{\partial^2 \theta}{\partial t^2} = 0, \quad (2)$$

$$EI \frac{\partial^4 \phi}{\partial x^4} - GJ \frac{\partial^2 \phi}{\partial x^2} + I_s \frac{\partial^2 \phi}{\partial t^2} - em \frac{\partial^2 v}{\partial t^2} = 0, \quad (3)$$

where EI , kGA , GJ and EI , respectively, are the bending, shear, torsional and warping rigidities, m is the mass per unit length, I_c is the mass moment of inertia of cross-section per unit length, and I_s is the polar moment of inertia per unit length with respect to the shear center.

Let

$$v(x, t) = V(x) \sin \omega t, \quad \theta(x, t) = \Theta(x) \sin \omega t, \quad \phi(x, t) = \Phi(x) \sin \omega t, \\ \zeta = x/L, \quad (4-7)$$

where ω is the angular frequency, V , Θ and Φ are the normal functions of v , θ and ϕ , respectively, and ζ is the non-dimensional co-ordinate. Substituting equations (4)–(7) into differential equations (1)–(3) leads to

$$\frac{kGA}{L^2} (V'' - \Theta' L) + m\omega^2 V - em\omega^2 \Phi = 0, \quad (8)$$

$$\frac{EI}{L^2} \Theta'' + \frac{kGA}{L} (V' - \Theta L) + I_c \omega^2 \Theta = 0, \quad (9)$$

$$\frac{EI}{L^4} \Phi'''' - \frac{GJ}{L^2} \Phi'' - I_s \omega^2 \Phi + em\omega^2 V = 0, \quad (10)$$

where a prime denotes differentiation with respect to the non-dimensional co-ordinate ζ . Introducing the following differential operators,

$$D = \frac{d}{d\zeta}, \quad L_{11} = \frac{kGA}{L^2} D^2 + m\omega^2, \quad L_{12} = -\frac{kGA}{L} D, \quad L_{13} = -em\omega^2, \\ L_{21} = \frac{kGA}{L} D, \quad L_{22} = \frac{EI}{L^2} D^2 - kGA + I_c \omega^2, \quad L_{23} = 0, \\ L_{31} = em\omega^2, \quad L_{32} = 0, \quad L_{33} = \frac{EI}{L^4} D^4 - \frac{GJ}{L^2} D^2 - I_s \omega^2, \quad (11)$$

equations (8)–(10) can be rewritten as

$$L_{11} V + L_{12} \Theta + L_{13} \Phi = 0, \quad L_{21} V + L_{22} \Theta + L_{23} \Phi = 0, \\ L_{31} V + L_{32} \Theta + L_{33} \Phi = 0. \quad (12-14)$$

The set of differential equations (12)–(14) can be shown [18] to imply that

$$\Delta V = 0, \quad \Delta \Theta = 0, \quad \Delta \Phi = 0, \quad (15)$$

where

$$\Delta = \begin{bmatrix} L_{11} & L_{12} & L_{13} \\ L_{21} & L_{22} & L_{23} \\ L_{31} & L_{32} & L_{33} \end{bmatrix}. \quad (16)$$

Setting the determinant of differential operator matrix (16) equal to zero leads to the following eighth order differential equation:

$$\{D^8 + (\kappa_2 - \kappa_1 + \kappa_3)D^6 - [\kappa_1(\kappa_2 + \kappa_3) - \kappa_2\kappa_3 + \kappa_4 + \kappa_5]D^4 - [\kappa_4(\kappa_2 + \kappa_3) + \kappa_1(\kappa_2\kappa_3 - \kappa_5) - \kappa_2\kappa_6]D^2 + (\kappa_6 - \kappa_4)(\kappa_2\kappa_3 - \kappa_5)\}R = 0. \quad (17)$$

Here R denotes V , Θ or Φ , and the non-dimensional parameters κ_1 – κ_6 are given by the following:

$$\kappa_1 = GJL^2/EI, \quad \kappa_2 = m\omega^2L^2/kGA, \quad \kappa_3 = I_c\omega^2L^2/EI, \quad (18-20)$$

$$\kappa_4 = I_s\omega^2L^4/EI, \quad \kappa_5 = m\omega^2L^4/EI, \quad \kappa_6 = e^2m\omega^2L^4/EI. \quad (21-23)$$

Taking a solution in the exponential form

$$R = e^{r\zeta} \quad (24)$$

and introducing the variable

$$s = r^2, \quad (25)$$

the following characteristic equation can be obtained from the differential equation (17):

$$s^4 + (\kappa_2 - \kappa_1 + \kappa_3)s^3 - [\kappa_1(\kappa_2 + \kappa_3) - \kappa_2\kappa_3 + \kappa_4 + \kappa_5]s^2 - [\kappa_4(\kappa_2 + \kappa_3) + \kappa_1(\kappa_2\kappa_3 - \kappa_5) - \kappa_2\kappa_6]s + (\kappa_6 - \kappa_4)(\kappa_2\kappa_3 - \kappa_5) = 0. \quad (26)$$

Using the technique employed by Bishop *et al.* [3], it may be shown that all four roots of equation (26) are real, non-zero, non-equal, two of them positive and two negative. The eight roots can be written as

$$r_1, \quad -r_1, \quad r_2, \quad -r_2, \quad r_3, \quad -r_3, \quad r_4, \quad -r_4, \\ r_1 = \sqrt{s_1}, \quad r_2 = \sqrt{s_2}, \quad r_3 = i\sqrt{s_3}, \quad r_4 = i\sqrt{s_4}, \quad (27)$$

where $i = \sqrt{-1}$.

Then the general solution of V , Θ and Φ can be written in the following form:

$$V(\zeta) = A_1 \cosh r_1 \zeta + A_2 \sinh r_1 \zeta + A_3 \cosh r_2 \zeta + A_4 \sinh r_2 + A_5 \cos r_3 \zeta \\ + A_6 \sin r_3 \zeta + A_7 \cos r_4 \zeta + A_8 \sin r_4 \zeta, \quad (28)$$

$$\Theta(\zeta) = B_1 \cosh r_1 \zeta + B_2 \sinh r_1 \zeta + B_3 \cosh r_2 \zeta + B_4 \sinh r_2 + B_5 \cos r_3 \zeta \\ + B_6 \sin r_3 \zeta + B_7 \cos r_4 \zeta + B_8 \sin r_4 \zeta, \quad (29)$$

$$\Phi(\zeta) = C_1 \cosh r_1 \zeta + C_2 \sinh r_1 \zeta + C_3 \cosh r_2 \zeta + C_4 \sinh r_2 + C_5 \cos r_3 \zeta \\ + C_6 \sin r_3 \zeta + C_7 \cos r_4 \zeta + C_8 \sin r_4 \zeta, \quad (30)$$

where A_1 – A_8 , B_1 – B_8 and C_1 – C_8 are three different sets of constants.

Substituting equations (28) and (29) into equation (9) yields the relations between the A 's and the B 's as follows:

$$B_1 = (\alpha_1/L)A_2, \quad B_2 = (\alpha_1/L)A_1, \quad B_3 = (\alpha_2/L)A_4, \quad B_4 = (\alpha_2/L)A_3, \\ B_5 = (\alpha_3/L)A_6, \quad B_6 = -(\alpha_3/L)A_5, \quad B_7 = (\alpha_4/L)A_8, \quad B_8 = -(\alpha_4/L)A_7. \quad (31)$$

Here the constants α_i , $i = 1, 2, 3, 4$, are given by

$$\alpha_m = \frac{\kappa_5 r_m}{\kappa_5 - \kappa_2 (r_m^2 + \kappa_3)}, \quad m = 1, 2; \quad \alpha_n = \frac{\kappa_5 r_n}{\kappa_5 + \kappa_2 (r_n^2 - \kappa_3)}, \quad n = 3, 4. \quad (32)$$

Similarly, substituting equations (28)–(30) into equation (8) gives the relations between the constant A 's and C 's.

$$\begin{aligned} C_1 &= (\lambda_1 / e\kappa_2)A_1, & C_2 &= (\lambda_1 / e\kappa_2)A_2, & C_3 &= (\lambda_2 / e\kappa_2)A_3, & C_4 &= (\lambda_2 / e\kappa_2)A_4, \\ C_5 &= (\lambda_3 / e\kappa_2)A_5, & C_6 &= (\lambda_3 / e\kappa_2)A_6, & C_7 &= (\lambda_4 / e\kappa_2)A_7, & C_8 &= (\lambda_4 / e\kappa_2)A_8, \end{aligned} \quad (33)$$

where

$$\lambda_j = \kappa_2 + r_j (r_j - \alpha_j), \quad j = 1, 2; \quad \lambda_k = \kappa_2 - r_k (r_k - \alpha_k), \quad k = 3, 4. \quad (34)$$

By imposing the boundary conditions, the constants A_1 – A_8 , and consequently B_1 – B_8 and C_1 – C_8 , can be calculated, as described in the following section.

3. BOUNDARY CONDITIONS AND FREQUENCY EQUATION

The necessary and sufficient boundary conditions for beams with clamped and free boundaries are as follows. For a clamped end,

$$V = 0, \quad \Theta = 0, \quad \Phi = 0, \quad \Phi' = 0. \quad (35)$$

For a free end,

$$\Theta'' + \kappa_3 \Theta = 0, \quad \Theta' = 0, \quad \kappa_1 \Phi' - \Phi''' = 0, \quad \Phi'' = 0. \quad (36)$$

For a clamped–free beam, application of boundary conditions (35) and (36) into equations (28)–(30) at $\zeta = 0$ and $\zeta = 1$ will yield eight linear homogeneous equations, which may be written in the matrix form

$$\mathbf{MA} = \mathbf{0}, \quad (37)$$

where vector \mathbf{A} contains the eight constants and \mathbf{M} is an 8×8 non-symmetric matrix, given by

$$\begin{bmatrix} 1 & 0 & 1 & 0 & 1 & 0 & 1 & 0 \\ 0 & \alpha_1^* & 0 & \alpha_2^* & 0 & \alpha_3^* & 0 & \alpha_4^* \\ \lambda_1^* & 0 & \lambda_2^* & 0 & \lambda_3^* & 0 & \lambda_4^* & 0 \\ 0 & \lambda_1^* r_1 & 0 & \lambda_2^* r_2 & 0 & \lambda_3^* r_3 & 0 & \lambda_4^* r_4 \\ \alpha_1^* \mu_1 Sh_1 & \alpha_1^* \mu_1 Ch_1 & \alpha_2^* \mu_2 Sh_2 & \alpha_2^* \mu_2 Ch_2 & \alpha_3^* \gamma_3 S_3 & \alpha_3^* \gamma_3 C_3 & \alpha_4^* \gamma_4 S_4 & \alpha_4^* \gamma_4 C_4 \\ \alpha_1^* r_1 Ch_1 & \alpha_1^* r_1 Sh_1 & \alpha_2^* r_2 Ch_2 & \alpha_2^* r_2 Sh_2 & -\alpha_3^* r_3 C_3 & -\alpha_3^* r_3 S_3 & -\alpha_4^* r_4 C_4 & -\alpha_4^* r_4 S_4 \\ \lambda_1^* r_1 \delta_1 Sh_1 & \lambda_1^* r_1 \delta_1 Ch_1 & \lambda_2^* r_2 \delta_2 Sh_2 & \lambda_2^* r_2 \delta_2 Ch_2 & -\lambda_3^* r_3 \epsilon_3 S_3 & \lambda_3^* r_3 \epsilon_3 C_3 & -\lambda_4^* r_4 \epsilon_4 S_4 & \lambda_4^* r_4 \epsilon_4 C_4 \\ \lambda_1^* r_1^2 Ch_1 & \lambda_1^* r_1^2 Sh_1 & \lambda_2^* r_2^2 Ch_2 & \lambda_2^* r_2^2 Sh_2 & -\lambda_3^* r_3^2 C_3 & -\lambda_3^* r_3^2 S_3 & -\lambda_4^* r_4^2 C_4 & -\lambda_4^* r_4^2 S_4 \end{bmatrix},$$

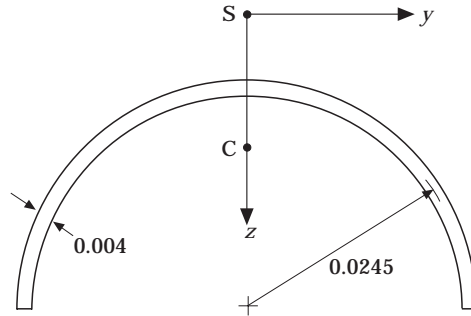


Figure 2. The cross-section and dimensions (in meters) of the beam studied in example I.

where

$$\alpha_i^* = \alpha_i / L, \quad \lambda_i^* = \lambda_i / e\kappa_2, \quad i = 1, 2, 3, 4, \quad (38)$$

$$Sh_j = \sinh r_j, \quad Ch_j = \cosh r_j, \quad \mu_j = \kappa_3 + r_j^2, \quad \delta_j = \kappa_1 - r_j^2, \quad j = 1, 2, \quad (39)$$

$$S_k = \sin r_k, \quad C_k = \cos r_k, \quad \gamma_k = r_k^2 - \kappa_3, \quad \varepsilon_k = \kappa + r_k^2, \quad k = 3, 4. \quad (40)$$

Non-trivial solutions are calculated by imposing

$$\det [\mathbf{M}(\omega)] = 0. \quad (41)$$

Equation (41) is the frequency equation, which can be numerically solved to give the values of ω that make the determinant singular.

4. NUMERICAL EXAMPLES

In this section the natural frequency analysis of section 2 is applied to three example problems, and the effects of warping stiffness, shear deformation and rotatory inertia on the coupled bending–torsional natural frequencies of cantilever beams are investigated.

4.1. EXAMPLE I

A thin walled uniform beam with a cross-section of an arc of a circle (Figure 2) is considered. It allows a comparison with the dynamic stiffness results of Friberg [11]. The properties of the beam are listed in Table 1.

The first five natural frequencies (in Hz) are obtained by including/excluding the effect of warping stiffness and are shown in Table 2, together with Friberg's [11] results, which are based on both Euler–Bernoulli and Vlasov beam theories, and the effect of warping is taken into consideration. Vlasov beam theory partially takes into account Timoshenko effects, by including the rotatory inertia but not shear deformation. The relative errors due to omission of warping and Timoshenko effects are shown in Figures 3 and 4, respectively. Since the warping stiffness is small, its inclusion does not greatly alter the frequencies of lower order modes. Given that the present beam is rather thin and the frequencies are not very high, except for the fifth mode, Timoshenko effects on the natural frequencies are insignificant. The corresponding mode shapes are shown in Figure 5. Note that in this figure and the following ones, the Θ and Φ components of the mode shapes have been

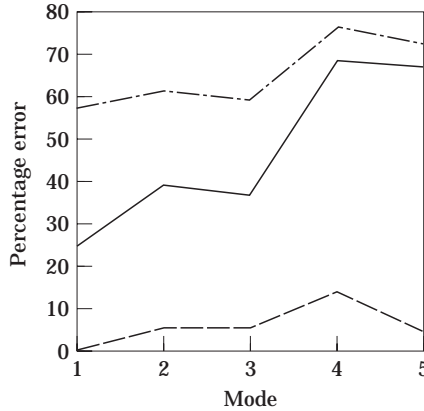


Figure 3. Percentage errors due to omission of the warping effect. —, Example I; ---, Example II; —·—, Example III.

TABLE 1

Property details of the three beams studied in the examples

	Example I	Example II	Example III
EI (N m ²)	6380	30.43×10^7	14.36×10^4
GJ (N m ²)	43.46	97.83×10^4	346.71
kGA (N)	4.081×10^6	52.82×10^7	20.81×10^6
EF (N m ⁴)	0.10473	81.58×10^5	536.51
I_s (kg m)	0.501×10^{-3}	56.87	3.17×10^{-2}
I_c (kg m)	0.251×10^{-3}	25.36	5.65×10^{-3}
m (kg/m)	0.835	225	4.256
L (m)	0.82	3.2	2.7
e (m)	0.0155	0.336	0.0735

TABLE 2

Natural frequencies (Hz) of cantilever semi-circular beam studied in Example I: (1) reference [11], Euler–Bernoulli theory; (2) reference [11], Vlasov theory; (3) present approach, including warping; (4) present approach, excluding warping

Modal index	Approach			
	(1)	(2)	(3)	(4)
1	63.79	63.76	63.51	63.39
2	137.7	137.5	137.39	129.34
3	278.4	278.2	275.82	259.22
4	484.8	483.9	481.10	415.72
5	663.8	657.3	639.76	607.29

multiplied by the distance e in order to compare Θ and Φ directly with the V component. For the first three modes, exclusion of warping or Timoshenko effects make no difference to the variations of bending displacement and torsional rotation; therefore mode shapes of Timoshenko model with warping are shown only in Figures 5(a)–(c) for these modes.

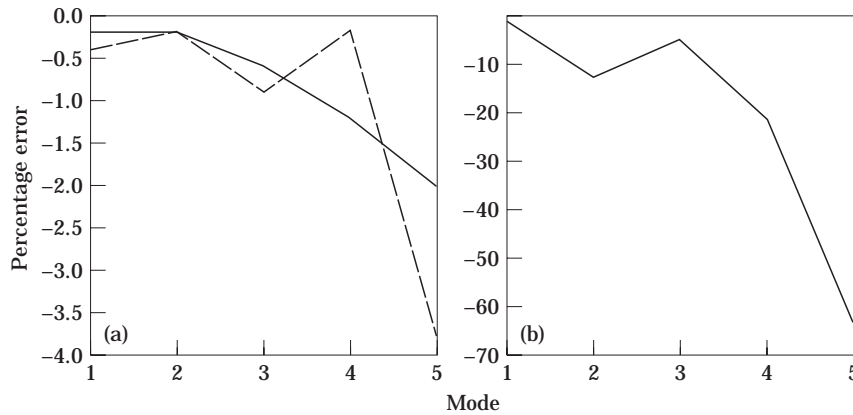


Figure 4. Percentage errors due to omission of Timoshenko effects. (a) Examples I and III (—, example I; ---, example III); (b) example II.

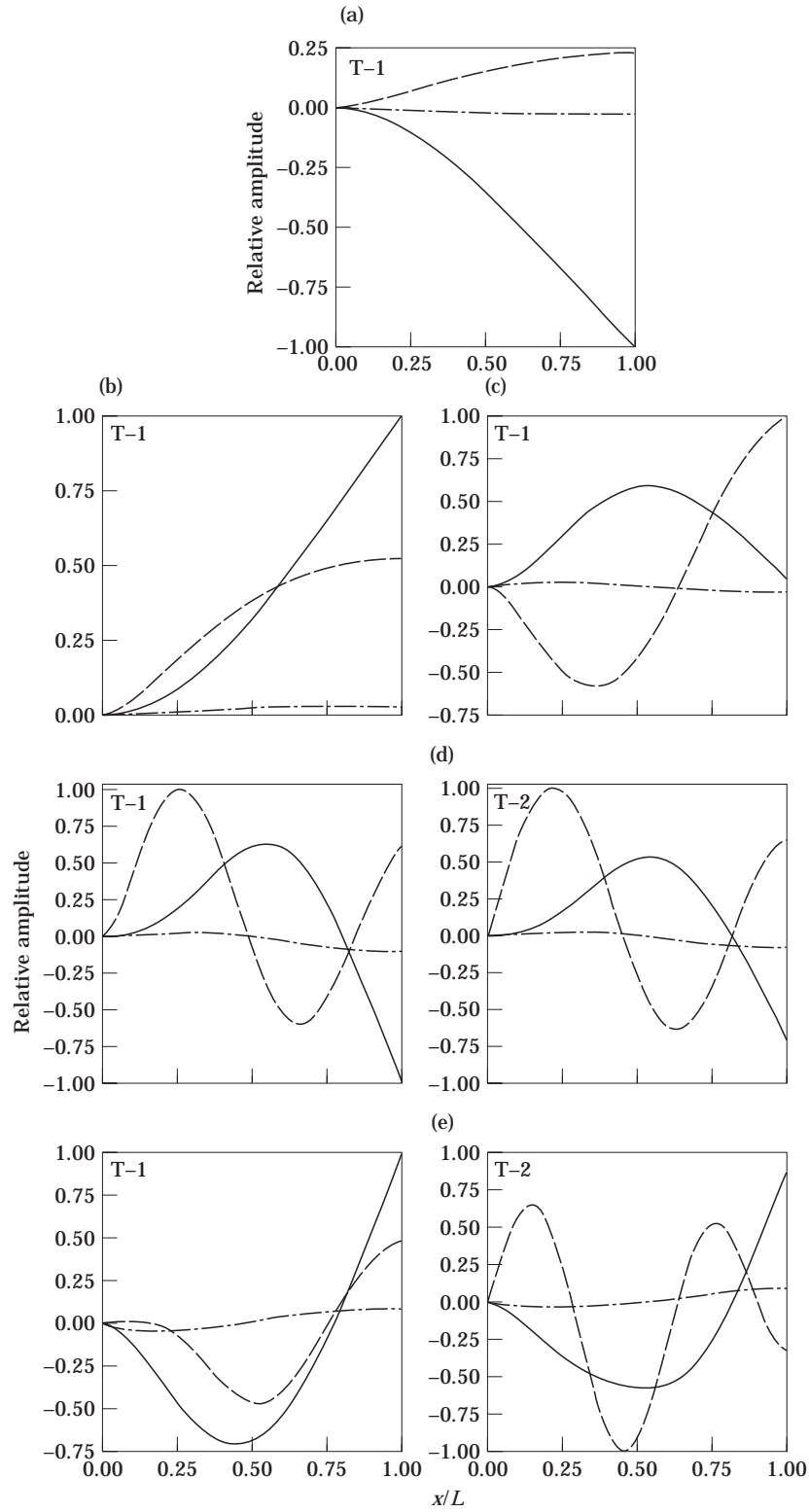


Figure 5. The mode shapes of example I. —, V ; ---, θ ; —·—, ϕ . T-1, Timoshenko model, including warping effect; T-2, Timoshenko model, excluding warping effect. (a) Mode 1; (b) mode 2; (c) mode 3; (d) mode 4; (e) mode 5.

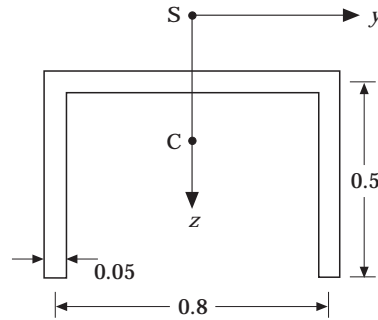


Figure 6. The cross-section and dimensions (in meters) of the beam studied in example II.

For the last two modes, mode shapes with and without warping differ and these are shown separately in Figures 5(d) and 5(e).

A relatively thick beam for which shear deformation and rotatory inertia effects are expected to be significant even at lower frequencies is given in the following example.

4.2. EXAMPLE II

This is the case of a concrete cantilever channel beam, shown in Figure 6, and the properties are given in column 2 of Table 1.

In Table 3 are shown the values of the first five modes, which are obtained by including warping effects in the Euler–Bernoulli model of reference [10] and the present Timoshenko model. An examination of Figures 3 and 4(b) reveals that both the warping and Timoshenko effects are quite significant for all of the natural frequencies, and errors arising from their omission are enormous. The mode shapes as given by the Euler–Bernoulli theory and Timoshenko theory, including/excluding warping are plotted in Figure 7. Relative measures of bending displacement and torsional rotation show that all of the modes are coupled modes. Although modes 2 and 5 are predominantly bending modes, when the effect of warping is excluded they become pure torsion modes. Another observation is that the fourth mode, which was a dominant torsion mode, has become a strongly coupled mode when the Timoshenko effects are considered.

TABLE 3

Natural frequencies (Hz) of cantilever channel beam studied in Example II: (1) reference [10], Euler–Bernoulli theory; (2) present approach, including warping; (3) present approach, excluding warping

Modal index	Approach		
	(1)	(2)	(3)
1	24.03	23.79	10.19
2	88.54	78.26	30.34
3	131.41	124.78	50.99
4	358.57	295.26	69.68
5	549.83	334.88	91.60

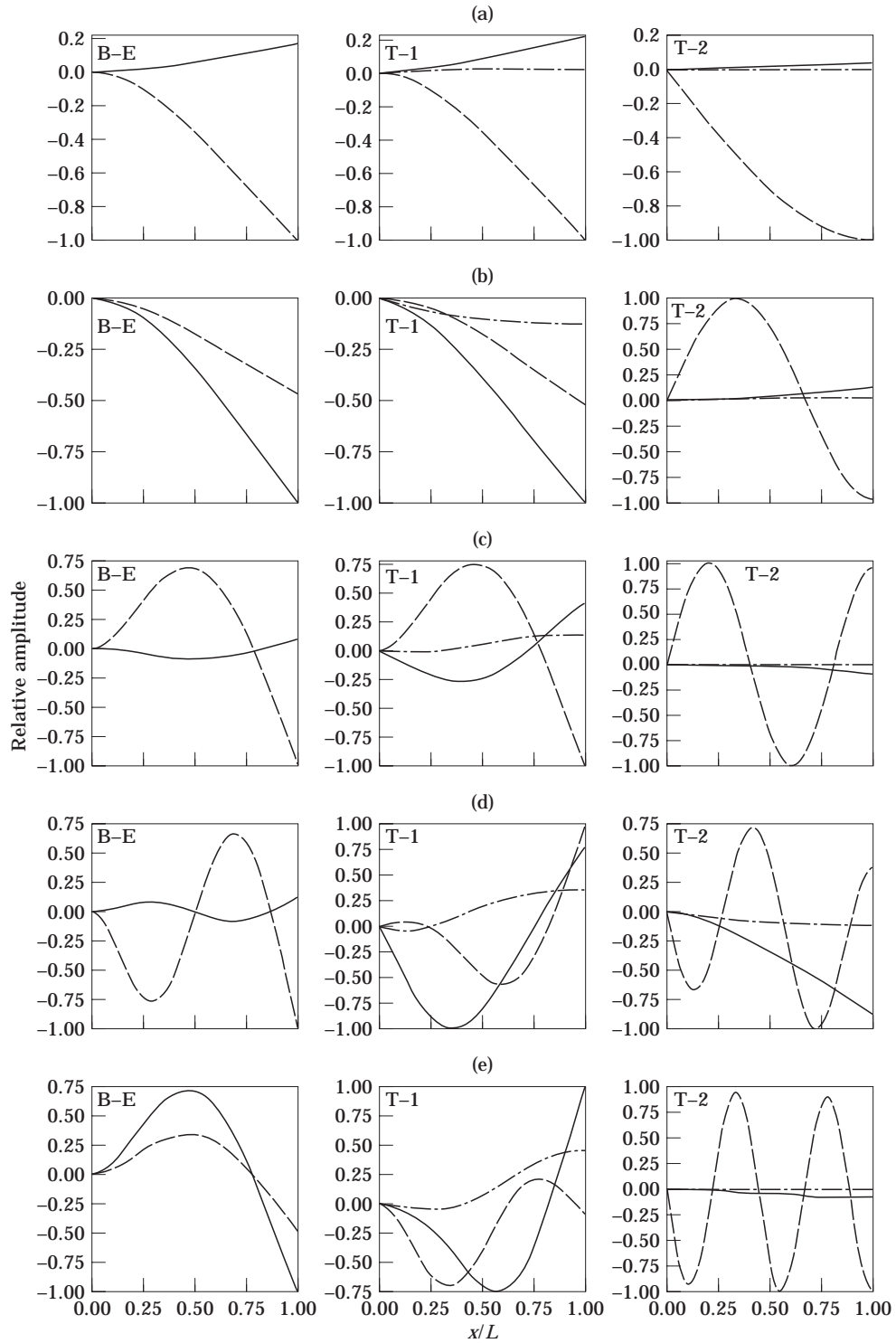


Figure 7. The mode shapes of example II. B-E, Euler-Bernoulli model; T-1, Timoshenko model, including warping effect; T-2, Timoshenko model, excluding warping effect. (a) Mode 1; (b) mode 2; (c) mode 3; (d) mode 4; (e) mode 5.

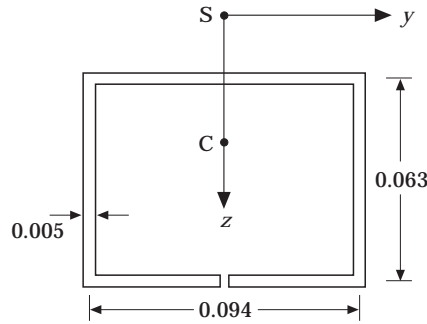


Figure 8. The cross-section and dimensions (in meters) of the beam studied in example III.

4.3. EXAMPLE III

The final example considers a thin-walled box beam with an axial slit along its length (Figure 8). Data of the beam are listed in Table 1, and the natural frequencies are tabulated in Table 4. While the effects of shear deformation and rotatory inertia are negligible, it is indicated in Figure 3 that the errors incurred are significant if no allowance is made for the warping stiffness. In Figure 9 is shown the variation of V , Θ and Φ along the length of the beam. Since the contribution of the Θ component is insignificant, the mode shapes based on the Euler–Bernoulli theory and Timoshenko theory are identical. For all of the modes, there is a strong coupling between bending displacement and torsional rotation. However, if the effect of warping is excluded, although for the first three modes strong coupling still exists, modes 4 and 5 become predominantly torsion modes, with a little contribution from bending.

5. CONCLUSIONS

The analysis of the natural vibrations of bending–torsion coupled Timoshenko beams has been presented taking into account the effects of warping stiffness, shear deformation and rotatory inertia. Three specific examples of beams with clamped–free end conditions are given to show the warping and Timoshenko effects. It is seen that when these effects are neglected, the errors associated with them become increasingly large as the beam

TABLE 4

Natural frequencies (Hz) of cantilever channel beam studied in Example III: (1) reference [10], Euler–Bernoulli theory; (2) present approach, including warping; (3) present approach, excluding warping

Modal index	Approach		
	(1)	(2)	(3)
1	11.03	11.01	8.30
2	39.02	38.93	23.79
3	58.19	57.82	36.63
4	152.39	150.51	47.21
5	209.38	205.32	67.15

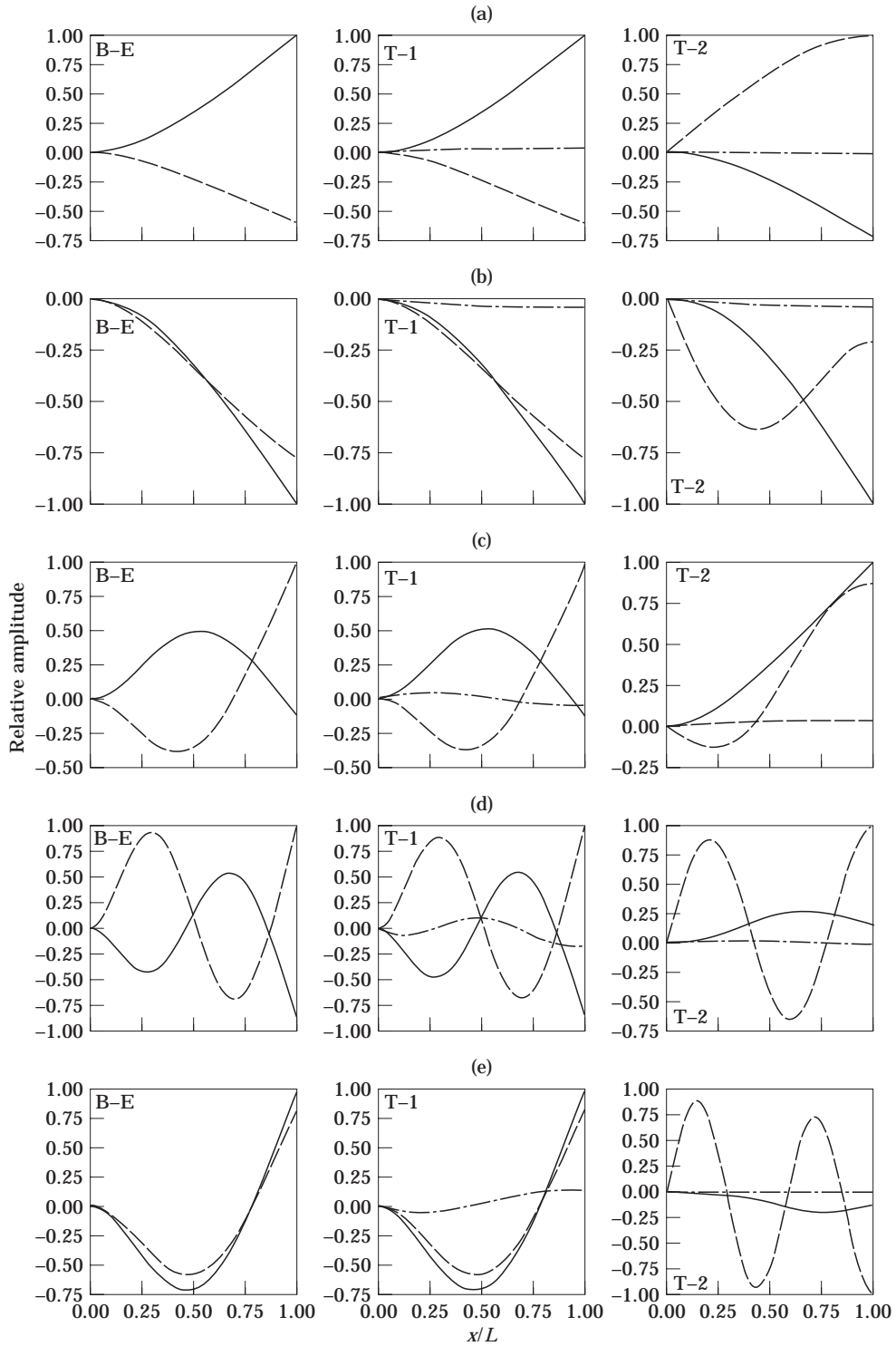


Figure 9. The mode shapes of example III. —, V ; ---, Θ ; —·—, Φ . B-E, Bernoulli–Euler model; T-1, Timoshenko model, including warping effect; T-2, Timoshenko model, excluding warping effect. (a) Mode 1; (b) mode 2; (c) mode 3; (d) mode 4; (e) mode 5.

thickness increases and as the modal index increases. The general effect of including warping is to increase the natural frequencies, while Timoshenko effects decrease them.

REFERENCES

1. P. O. FRIBERG 1983 *International Journal for Numerical Methods in Engineering* **19**, 479–493. Coupled vibrations of beams—an exact dynamic element stiffness matrix.
2. E. DOKUMACI 1987 *Journal of Sound and Vibration* **119**, 443–449. An exact solution for coupled bending and torsion vibrations of uniform beams having single cross-sectional symmetry.
3. R. E. D. BISHOP, S. M. CANNON and S. MIAO 1989 *Journal of Sound and Vibration* **131**, 457–464. On coupled bending and torsional vibration of uniform beams.
4. J. R. BANERJEE, S. GUO and W. P. HOWSON 1996 *Computers and Structures* **59**, 612–621. Exact dynamic stiffness matrix of a bending–torsion coupled beam including warping.
5. J. R. BANERJEE 1989 *International Journal for Numerical Methods in Engineering* **28**, 1283–1289. Coupled bending–torsional dynamic stiffness matrix for beam elements.
6. J. R. BANERJEE 1991 *Advances in Engineering Software* **13**, 17–24. A FORTRAN routine for computation of coupled bending–torsional dynamic stiffness matrix of beam elements.
7. J. R. BANERJEE and S. A. FISHER 1992 *International Journal for Numerical Methods in Engineering* **33**, 739–751. Coupled bending–torsional dynamic stiffness matrix for axially loaded beam elements.
8. J. R. BANERJEE and F. W. WILLIAMS 1994 *Journal of Sound and Vibration* **176**, 301–306. Clamped–clamped natural frequencies of a bending–torsion coupled beam.
9. M. J. KLAUSBRUCKNER and R. J. PRYPUTNIEWICZ 1995 *Journal of Sound and Vibration* **183**, 239–252. Theoretical and experimental study of coupled vibrations of channel beams.
10. M. TANAKA and A. N. BERCIN (to appear) *Computers and Structures*. Free vibration solution for uniform beams of nonsymmetrical cross section using Mathematica.
11. P. O. FRIBERG 1985 *International Journal for Numerical Methods in Engineering* **21**, 1205–1128. Beam element matrices derived from Vlasov’s theory of open thin-walled elastic beams.
12. A. Y. T. LEUNG 1991 *Thin Walled Structures* **11**, 431–438. Natural shape functions of compressed Vlasov element.
13. A. Y. T. LEUNG 1992 *Thin Walled Structures* **14**, 209–222. Dynamic stiffness analysis of thin-walled structures.
14. E. N. DVORKIN, D. CELENTANO, A. CUITINO and G. GIOIA 1989 *Computers and Structures* **33**, 187–196. A Vlasov beam element.
15. R. E. D. BISHOP and W. G. PRICE 1977 *Journal of Sound and Vibration* **50**, 469–477. Coupled bending and twisting of a Timoshenko beam.
16. J. R. BANERJEE and F. W. WILLIAMS 1992 *Computers and Structures* **42**, 301–310. Coupled bending–torsional dynamic stiffness matrix for Timoshenko beam elements.
17. J. R. BANERJEE and F. W. WILLIAMS 1994 *International Journal of Solids and Structures* **31**, 749–762. Coupled bending–torsional dynamic stiffness matrix of an axially loaded Timoshenko beam element.
18. F. B. HILDEBRAND 1976 *Advanced Calculus for Applications*. Englewood Cliffs, New Jersey: Prentice-Hall; second edition.